

This is a repository copy of *Commercially-Relevant Orthogonal Multi-Component Supramolecular Hydrogels for Programmed Cell Growth*.

White Rose Research Online URL for this paper:

<https://eprints.whiterose.ac.uk/133509/>

Version: Accepted Version

Article:

Vieira, Vania Margarida Pinto, Lima, Ana Catarina, de Jong, Menno et al. (1 more author) (2018) Commercially-Relevant Orthogonal Multi-Component Supramolecular Hydrogels for Programmed Cell Growth. *Chemistry : A European Journal*. pp. 15112-15118. ISSN 0947-6539

<https://doi.org/10.1002/chem.201803292>

Reuse

Items deposited in White Rose Research Online are protected by copyright, with all rights reserved unless indicated otherwise. They may be downloaded and/or printed for private study, or other acts as permitted by national copyright laws. The publisher or other rights holders may allow further reproduction and re-use of the full text version. This is indicated by the licence information on the White Rose Research Online record for the item.

Takedown

If you consider content in White Rose Research Online to be in breach of UK law, please notify us by emailing eprints@whiterose.ac.uk including the URL of the record and the reason for the withdrawal request.

Commercially-Relevant Orthogonal Multi-Component Supramolecular Hydrogels for Programmed Cell Growth

Vânia M. P. Vieira,^[a] Ana C. Lima,^[b] Menno de Jong,^[b] David K. Smith^{*[a]}

Abstract: This paper reports the ability of synthetically-simple, commercially-viable sugar-derived 1,3:2,4-dibenzylidenesorbitol-4',4''-diacylhydrazide (DBS-CONHNH₂) to support cell growth. Simple mixing and orthogonal self-sorting can formulate heparin, agarose, and heparin-binding micelles into these gels – easily incorporating additional function. Interestingly, the components used in the gel formulation, direct the ability of cells to grow, meaning the chemical programming of these multi-component gels is directly translated to the biological systems in contact with them. This simple approach has potential for future development in regenerative medicine.

Introduction

Hydrogels have great potential in regenerative medicine and tissue engineering,^[1] primarily as a result of their rheological similarities to the extracellular matrix, and their ability to be tuned using chemical synthesis.^[2] Polymer gels (PGs) have been widely exploited in this regard.^[1a,b,3] In recent years, however, there has been increasing interest in hydrogels that self-assemble from low-molecular-weight gelators (LMWGs) as a result of non-covalent interactions between molecular-scale building blocks.^[4] Such materials can be easily tuned at the molecular level via simple organic synthesis, and are reversible as a result of the self-assembly event. However, the use of LMWGs in tissue culture is much rarer than PGs.^[5] Most commonly, the LMWGs applied are based on relatively complex, self-assembling peptides with high molecular weights (>1000 Da); excitingly such systems have been shown to have regenerative medicine potential *in vivo* in animal model systems.^[6] However, reports of simpler LMWGs (<500 Da) in tissue engineering are even rarer. In early work, 9-fluorenylmethoxycarbonyl-dipeptide hydrogels were used,^[7] with Ulijn and co-workers demonstrating the advantages of co-assembly with Fmoc-RGD (arginine-glycine-aspartic acid) tripeptide to interact with anchorage-dependent cells.^[8] There have been other reports of peptide gelators with the goal of tuning biological outcomes through chemical functionality and

rheological performance.^[9] Hamachi and co-workers used an amino acid derivative gelator and patterned it by etching with a laser to encourage spatially controlled cell growth.^[10] Perhaps surprisingly, there have been very limited reports of functional groups other than amino acids/peptides as LMWGs in tissue engineering, and given the amyloid-forming nature of many peptide gelators^[5b] there is a significant need to explore other systems for potential *in vivo* use. Simple amide hydrogelators were used by Feng and co-workers – the chirality of the gelator impacted on tissue growth and incorporating a photo-active unit introduced photo-responsiveness.^[11] Moving away from amides, Barthélémy and co-workers elegantly applied nucleobase-derived gels with human mesenchymal stem cells – cell survival was dependent on gelator structure.^[12] This gelator was used in combination with collagen to create hybrid materials.^[13] Others have also made use of guanosine-derived gels for cell culture.^[14] Surprisingly, given their biological importance, there are very few examples of sugar-based LMWGs being used for tissue culture. There are limited examples of peptides modified with sugars,^[15] and Barthélémy's nucleobase gelators contain sugar units,^[12,13] but other sugar-containing gelators applied in tissue engineering remain very rare.^[16]

In this work, we wanted to demonstrate a commercially-viable approach to simple self-assembled tissue culture materials. We selected gels based on sugar-derived gelator 1,3:2,4-dibenzylidenesorbitol (DBS), an organogelator used in bulk-scale in the chemical industry, in (e.g.) personal care products and polymer clarification.^[17] We have developed hydrogelator versions of DBS,^[18] made via simple two-step synthesis using cheap bulk chemicals and inherently-scalable industrially-relevant methods. Here, we combine one of these simple, commercially-relevant hydrogels with a multi-component approach to incorporate other units that can add useful functionality via mixing. Self-sorting within gels that contain a mixture of components, to yield materials capable of orthogonal function has emerged as one of the key advantages of using LMWGs.^[19]

We previously reported multi-component hydrogels based on a different gelator 1,3:2,4-dibenzylidene-D-sorbitol-*p,p'*-dicarboxylic acid (DBS-COOH),^[20] but these were not stable above pH 5.5, and were unsuitable for tissue culture. For this study, we focussed attention on 1,3:2,4-dibenzylidene-D-sorbitol-*p,p'*-diacylhydrazide (DBS-CONHNH₂, Fig. 1), which is stable from ca. pH 2.5-11.5. We aimed to combine this LMWG with agarose PG (to provide greater robustness), heparin (to assist angiogenesis and growth factor promotion),^[21] and self-assembling C₁₆-DAPMA micelles (to bind heparin and control its release).^[22] In this way, we hoped to easily generate multi-functional gels compatible with tissue culture, opening up potential low cost regenerative medicine applications.

[a] Prof. D. K. Smith and Dr V. M. P. Vieira
Department of Chemistry
University of York
Heslington, York, YO10 5DD, UK.
E-mail: david.smith@york.ac.uk

[b] Dr M. de Jong and Dr A. C. Lima
Nano Fiber Matrices
Groningen
The Netherlands

Supporting information for this article is given via a link at the end of the document.

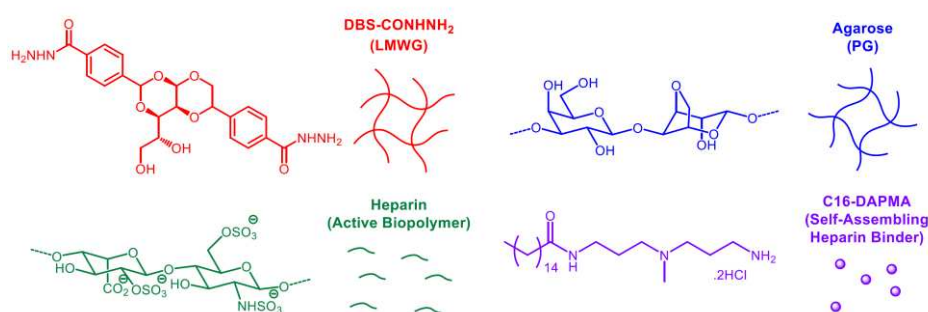


Figure 1. Components used to formulate the self-assembled gels studied in this paper – low-molecular-weight gelator, DBS-CONHNH₂; polymer gelator, agarose; bioactive heparin and self-assembling micellar heparin binder, C16-DAPMA.

Results and Discussion

Hydrogelator DBS-CONHNH₂ was synthesised in very good yield using methods reported previously^[18b] and demonstrated to form gels in aqueous Tris-HCl buffer (pH 7.4, 10 mM) and NaCl (150 mM) at a loading of 0.4% wt/vol in water, with a T_{gel} value of 86°C. The impact of the presence of heparin on the gelation event was then tested.

In all cases, DBS-CONHNH₂ still assembled into a gel (tested up to 1 mM heparin, 0.67 wt/vol%), with equivalent T_{gel} values of 83–86°C. Infrared (IR) analysis indicated that the spectrum for the DBS-CONHNH₂-heparin xerogel was equivalent to the sum of the individual spectra (Fig. S1, see ESI for more detailed discussion). Circular dichroism (CD) spectroscopy indicated a similar spectrum associated with self-assembled DBS-CONHNH₂ with or without heparin, suggesting the two

components are largely independent of one another (Fig. 2C). In each case, the peak maximum is at 275 nm, with similar ellipticities of 82 and 68 mdeg respectively. The kinetics of assembly were also very similar in the absence and presence of heparin as monitored by time-resolved CD spectroscopy (Fig. 2C), with self-assembly being effectively complete after ca. 3 minutes. TEM and SEM imaging of the DBS-CONHNH₂ gel indicated the presence of twisted and branched nanofibers (Figs. 2A and S7). In the presence of heparin, the nanofibre morphologies were very similar, with unspecific aggregates corresponding to heparin also being observed (Figs. 2B and S8). Rheology on the gel alone and in the presence of 1 mM heparin gave equivalent linear viscoelastic regions (LVR) extending to ca. 2.5% strain, and the G' values were very similar, indicating limited effect of heparin on the overall network (Figs. 3A and S13).

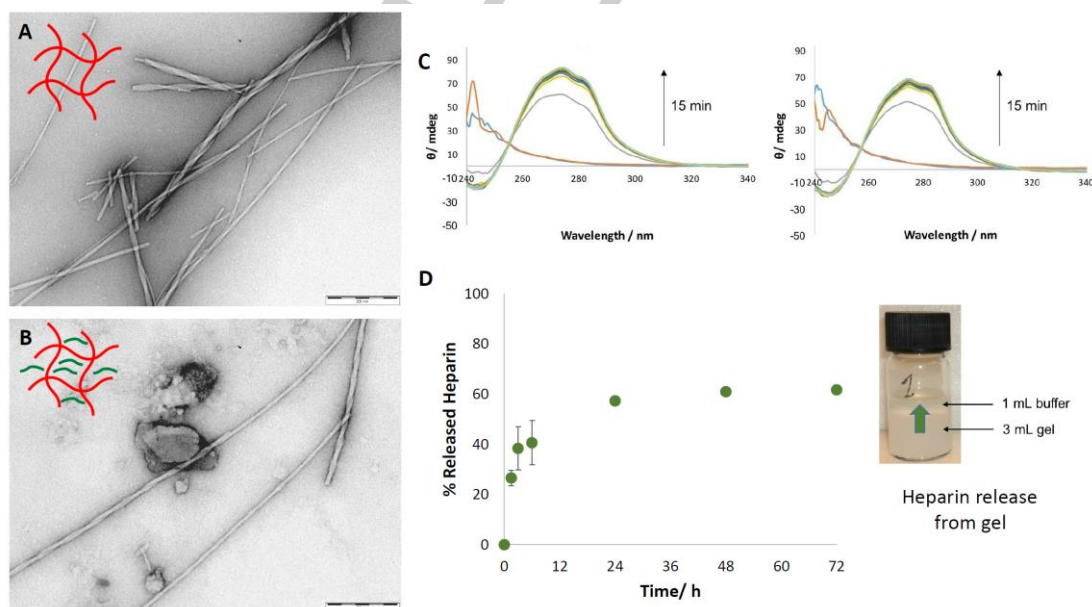


Figure 2. A) TEM image of DBS-CONHNH₂; scale bar, 200 nm; B) TEM image of DBS-CONHNH₂ in the presence of heparin; scale bar, 200 nm; C) Time resolved CD spectroscopy, with one spectrum measured every 60 s, following the assembly of DBS-CONHNH₂ (0.12% wt/vol) in the absence (left) and presence (right) of heparin (38 μ M) indicating that after the first two time-points (orange and blue lines), DBS-CONHNH₂ assembly is switched on and the peak at 275 nm associated with the self-assembled state is observed; D) Heparin release from DBS-CONHNH₂ hydrogel (0.4% wt/vol) loaded with heparin (1 mM).

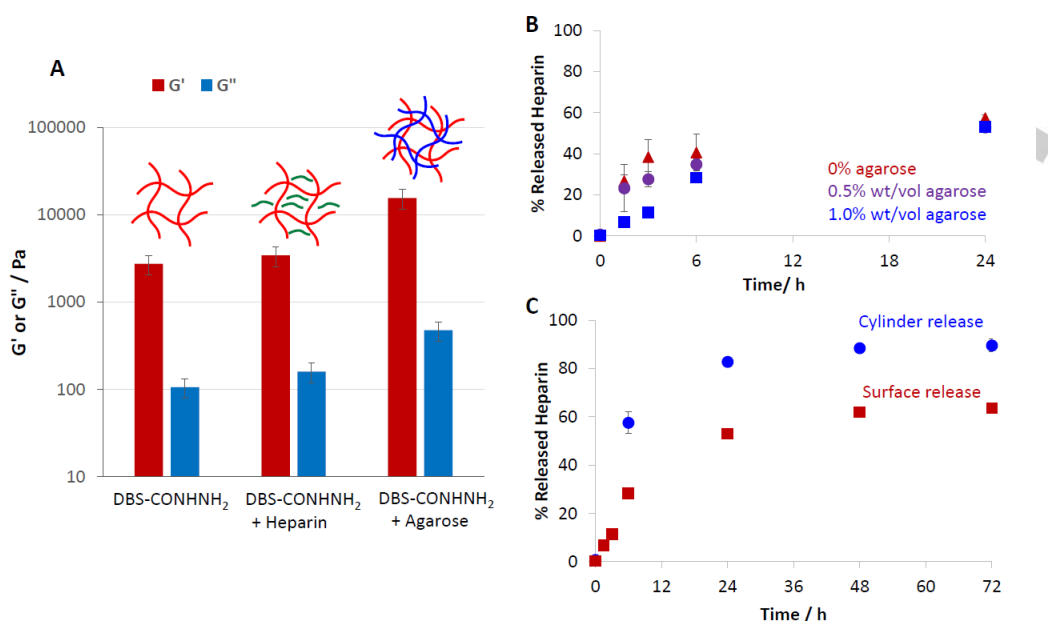


Figure 3. A) Summary of G' and G'' rheological data for 0.4% wt/vol DBS-CONHNH₂ alone and in the presence of heparin (1 mM) or agarose (1.0% wt/vol) indicating gel stiffening achieved by the addition of agarose; B) Release of heparin from DBS-CONHNH₂ gel surfaces (0.4% wt/vol) in the presence of varying agarose loadings (0% wt/vol, 0.5% wt/vol and 1.0% wt/vol); C) Release of heparin from DBS-CONHNH₂ hydrogel (0.4% wt/vol) and agarose (1% wt/vol) containing heparin (1 mM), either using buffer on top of the gel for 'surface release' or making a free-standing gel for 'cylinder release'.

We tested the ability of the network to release heparin, using methods that mimic cell culture conditions. A small amount of aqueous medium was placed on top of the gel and heparin release into it was quantified using a heparin-sensitive dye, Mallard Blue.^[23] Pleasingly, heparin release was observed – for a gel containing 1 mM heparin, 62% was released after 72 hours, with most of the release occurring in the first 24 hours (Fig. 2D). This is therefore a very simple method to formulate supramolecular gels capable of heparin release.

Agarose was then mixed into the gelation system – this PG offers a way to endow LMWGs with greater robustness by forming a PG/LMWG hybrid hydrogel.^[18a,24,25] In the presence of 1% wt/vol agarose, the DBS-CONHNH₂ gel has greater stiffness (ca. 15000 Pa, Fig. 3A). On further addition of heparin into this gel the stiffness fell back to 3800 Pa, indicating little impact of the agarose on gel stiffness in this case (Fig. S12), but strain resistance increased significantly (Fig. S13). This reflects the much greater ease of handling of the materials including agarose. The presence of agarose did not significantly affect DBS-CONHNH₂ assembly as monitored by CD spectroscopy (Figs. S3 and S4) – once again the peak shape was similar with a maximum at ca. 275 nm and an ellipticity of 50 mdeg.

The presence of agarose did not affect the total amount of heparin release, with 62% release under our experimental conditions observed over 48 hours (Fig. 3B). However, the agarose loading modified release kinetics in the first 6 hours, which slowed down in the presence of 0.5% wt/vol agarose, and even more so with 1.0% wt/vol agarose, suggesting that heparin diffusion is slower within the hybrid gel. The ease of handling of the hybrid hydrogel allowed us to also test heparin release from a self-standing cylinder of gel – the greater surface area and the

larger receiving volume, enhanced the kinetics of heparin release (doubling the initial rate of release) and increased the total amount of heparin released to 90% (Fig. 3C).

To control heparin, we also added C₁₆-DAPMA, previously reported by us as a self-assembling multivalent (SAMul) heparin binder,^[22] into the gels. At concentrations of C₁₆-DAPMA up to 1.2 mM, the DBS-CONHNH₂ hydrogel remained stable, with a T_{gel} of 83–86°C, the IR reflecting an overlap of the spectra of the individual components (Fig. S1), and minimal impact on the CD spectrum of DBS-CONHNH₂ (Fig. S2) suggesting that the self-assembled micelles do not adversely impact the self-assembly of the gel nanofibres (in contrast to our previous studies with DBS-COOH).^[20] TEM demonstrated the independent existence of DBS-CONHNH₂ nanofibres and C₁₆-DAPMA micelles (Fig. 4A). Rheology indicated that the presence of micelles had limited impact on gel stiffness, with G' remaining similar, but the stability towards strain reduced to 1%.

Heparin was then also added, with the intention it would interact with self-assembled C₁₆-DAPMA, becoming trapped in the gel. At 0.4 mM heparin, the gel remained stable with up to 1.6 mM C₁₆-DAPMA, but the T_{gel} values fell to ca. 66°C, indicating some impact on the nanoscale network. The CD intensity associated with DBS-CONHNH₂ was also lower (Fig. S2). TEM visualised both DBS-CONHNH₂ nanofibres, and the semi-crystalline nanostructures distinctive of complexes between C₁₆-DAPMA and heparin (Figs. 4B, S5 and S6).^[22b] However, in addition, it was also possible to identify some larger aligned structures (ca. 900 ± 200 nm) that resembled needles (Fig. 4C). Closer inspection, supported by SEM (Figs. S9 and S10) indicated rigid alignment/crystallisation of gel nanofibers. We suggest this is induced by the highly organised semi-crystalline

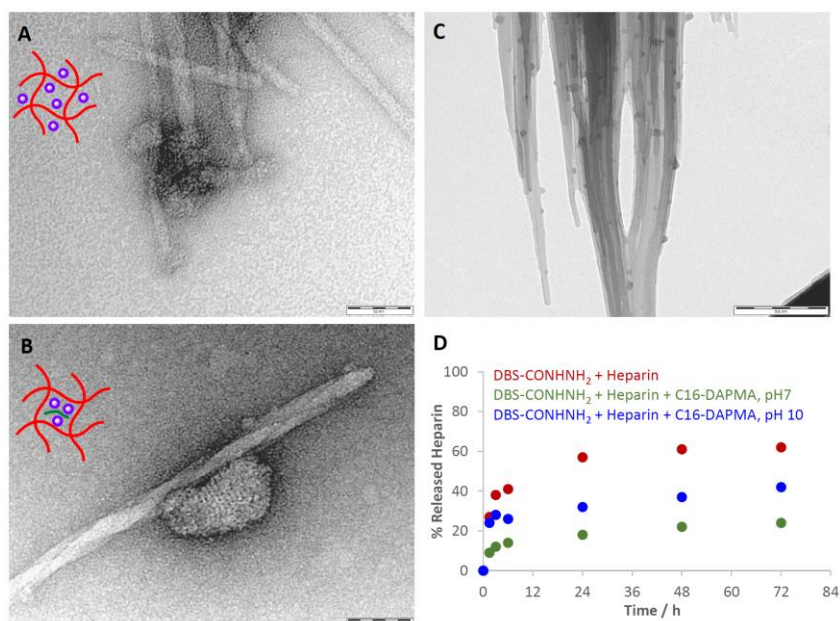


Figure 4. A) TEM image of DBS-CONH₂ in the presence of C16-DAPMA (scale bar, 50 nm); B) TEM image of DBS-CONH₂ in the presence of C16-DAPMA and heparin showing hierarchical nanoscale assemblies formed via complexation between C16-DAPMA cationic micelles and anionic heparin (scale bar, 50 nm); C) TEM image of aligned larger DBS-CONH₂ nanofibres also observed in the presence of C16-DAPMA and heparin (scale bar, 500 nm); D) controlled release of heparin from multi-component self-sorted gels, C16-DAPMA (2 mM) limits heparin (1 mM) release from DBS-CONH₂ (0.4% wt/vol) as a result of complexation. On raising pH from 7 to 10, complexation is disrupted to some extent, and greater heparin release is switched on.

hierarchical nanostructures formed when C16-DAPMA interacts with heparin. The presence of these structures did not, however, appear to have a major impact on the rheological performance of the gel. The incorporation of C16-DAPMA into the gel significantly lowered heparin release, with only 24% being released after 72 hours (Fig. 4D). Raising the pH of the receiving solution to pH 10 (borax/NaOH) increased the amount of heparin released over 72 hours to 42% (Fig. 4D) - the elevated pH deprotonates C16-DAPMA, disrupting its interactions with heparin and hence switching-on heparin release.

We tested this family of gels in tissue culture experiments using mouse embryonic fibroblast (3T3) cells to determine their biocompatibility, and uncover the impact of each individual component on cell growth. In this way, we hoped to learn how chemical programming, can direct biological outcomes.

Initially, we performed experiments in which the cells were grown on the gels (Fig. S15). Microscopy was challenging as a result of the gels being not completely optically transparent. The metabolic activity of the cells, using a cell density of 50000 cells/mL, on top of DBS-CONH₂ hydrogels was studied using cell proliferation reagent WST-1, and indicated that the cells grew effectively on DBS-CONH₂ - similar to or better than a control in which the cells were simply grown in medium in the well (Fig. S16-S18). In the presence of relatively high concentrations of heparin (667 and 1330 µg/mL), cell growth was inhibited - indeed by day 5, cell growth was just 10-15% of that observed on DBS-CONH₂ alone. This agrees with literature reports in which high concentrations of heparin inhibit cell growth.^[26] However, in these

initial experiments, there was a decrease in metabolic activity between days 5 and 7 because cell confluence had been reached, and the system was overloaded, leading to loss of adhesion and cell death. We therefore optimised the experimental conditions by lowering the cell density and used lower loadings of heparin. In these optimised conditions, the growth of cells on DBS-CONH₂ was very good - the metabolic activity of the cells was compared on days 1, 3 and 7, and a significant increase in metabolic activity was observed, particularly between days 3 and 7 (Fig. 5). To ensure the cells were adhering to the DBS-CONH₂ hydrogel surface and not migrating into the well, a cell migration assay was performed by simply preparing DBS-CONH₂ hydrogels (100 µL, 80 µL and 60 µL to test different gel thicknesses) in transwell inserts, and adding cells to the top of the gel (Figs. S30 and S31). If the cells migrate they will cross the membrane and adhere to the bottom of the well, which could be followed by optical microscopy - no cells were detected on the bottom of the DBS-CONH₂-loaded wells. This proves that the metabolic activities correspond to cells attached to the surface of DBS-CONH₂ hydrogels.

On mixing low concentrations of heparin (10 µg/mL, 25 µg/mL and 50 µg/mL) into DBS-CONH₂, the metabolic activity of the cells was consistently higher at day 7 (ca. 20-35%). This suggests that heparin release can enhance cell growth. The hybrid hydrogel containing DBS-CONH₂ and agarose was tested and cell growth was ca. 20% lower by day 7. Furthermore, the cell culture clearly struggled to establish itself with lower metabolic activity at days 1 and 3. When cell growth on a pure

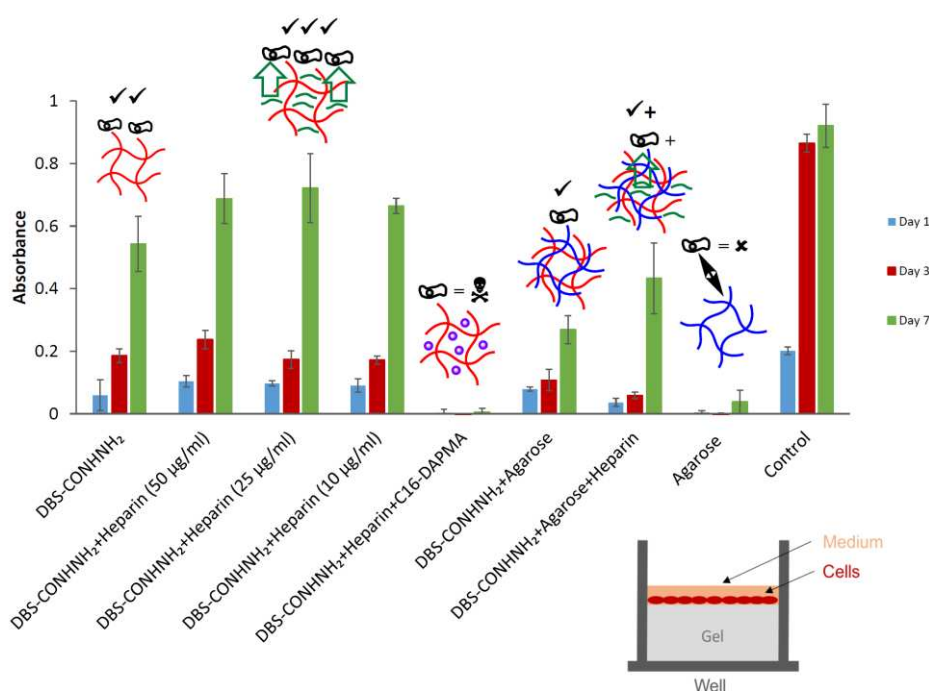


Figure 5. Absorbance of WST-1 reagent at 440 nm with (from left to right): DBS-CONHNH₂ hydrogel; DBS-CONHNH₂ hydrogel with heparin (50 µg/mL, 25 µg/mL and 10 µg/mL); DBS-CONHNH₂ hydrogels with heparin (50 µg/mL) and C₁₆-DAPMA (140 µg/mL); DBS-CONHNH₂ hydrogels with agarose (1% wt/vol); DBS-CONHNH₂ hydrogels with agarose (1% wt/vol) and heparin (50 µg/mL); agarose alone (1% wt/vol) and positive control (medium with cells). Cells are grown on top of the gels and monitored at day 1, 3 and 7. Schematic images indicate compositions of hybrid materials and outcomes of structural modification on cell growth.

agarose gel was tested, almost none was observed. Although agarose is known for being biocompatible and having mechanical properties suitable for cell culture, one of its main limitations relates to the fact that it does not contain moieties associated with cellular adhesion resulting in low cell proliferation.^[27] It is therefore interesting that in the hybrid LMWG/PG gel, reasonable cell growth is observed. This suggests that DBS-CONHNH₂ endows the hybrid gel with cell adhesion potential, whilst agarose provides it with robustness and ease-of-handling, and 'self-standing' capacity, facilitating the formation of gel scaffolds of different shapes. This demonstrates how low cost self-assembling additives such as DBS-CONHNH₂ can add significant function and value to PG systems by simple mixing.

When using gels containing C₁₆-DAPMA and heparin, cell growth was completely inhibited. We reasoned this was a result of cationic surfactant C₁₆-DAPMA leaching from the gel (see below for further proof), disrupting cell membranes, showing the limitations of this system.^[28]

As important control experiments, cells were grown in wells, which had gels placed into transwell inserts placed on top of the medium (Fig. S19), to understand the cytocompatibility of the gels and the impact of additives within the gel, which can be released into the cell growth medium to modify cell growth. Studies using WST-1 (Fig. S20) clearly demonstrated that, as before, cells grown in the presence of heparin showed small increases in metabolic activity (ca. 15%), indicative of beneficial effects of heparin release into the growth medium. Conversely, cells grown

in the presence of C₁₆-DAPMA and heparin were completely inhibited. When the gel combining just DBS-CONHNH₂ and C₁₆-DAPMA, was tested, cell growth was once again completely prevented, clearly indicating that C₁₆-DAPMA is released from these gels and is toxic to cell growth. Interestingly, in this assay, agarose had no adverse impact on cell growth, supporting the view that in the previous assays, agarose was not inhibiting cell growth through any toxicity effect, but simply because cells cannot adhere. Optical microscopy indicated effective cell growth in the presence of all DBS-CONHNH₂ gels except those containing C₁₆-DAPMA (Figs. S21-S23), successful MitoTracker staining indicated no damage to the membrane or reduced membrane potential (Figs. S24-26) and live/dead staining experiments (Figs S27-S29) demonstrated that cells successfully grow in the presence of these gels.

Conclusions

In summary, this study demonstrates that DBS-CONHNH₂ is a biocompatible low-molecular-weight hydrogelator that supports cell growth. Given the simple synthesis of this gelator, feasible on large scale using commercially-relevant methods, this system has considerable potential for application in tissue engineering and regenerative medicine. Furthermore, other nanosystems can be incorporated in the gel in a simple low-cost manner – specifically in this case, agarose, heparin and C₁₆-DAPMA. In

each case, we characterised these largely-orthogonal self-sorted materials and also explored the impact of additives on tissue culture. Specifically, heparin can be released from the gel, which appears to have beneficial effects on cell culture even with simple 3T3 cells. Agarose makes the gels more robust and easy to handle, but lowers the ability of cells to adhere to the gel. However, in the hybrid LMWG/PG gel formed by DBS-CONHNH₂ with agarose, cell growth occurs – i.e., both components play an active role – agarose providing robustness and DBS-CONHNH₂ enabling cell growth. Finally, the addition of C₁₆-DAPMA limits release of heparin by binding to it. However, gels incorporating C₁₆-DAPMA are not compatible with tissue growth owing to it leaching from the gel and being cytotoxic.

Overall, we have presented a simple low-cost approach to tissue engineering, and shown how a simple LMWG can be combined orthogonally with different additives, with the chemical inputs being able to program the biological outputs. We propose that this approach may underpin developments in regenerative medicine, and offers a highly tunable strategy by which LMWGs can be optimised for use in, and control of, a biological setting.

Acknowledgements

We thank European Commission Marie Curie ITN 316656 SMARTNET (VMPV and ACL) for funding. TEM and SEM imaging was performed by Meg Stark, Department of Biology, University of York.

Keywords: cell • gel • self-assembly • supramolecular

- [1] a) K. Y. Lee, D. J. Mooney, *Chem. Rev.*, **2001**, *101*, 1869–1880; b) J. A. Hunt, R. Chen, T. van Veen, N. Bryan, *J. Mater. Chem. B*, **2014**, *2*, 5319–5338; c) M. J. Webber, E. A. Appel, E. W. Meijer, R. Langer, *Nature Mater.*, **2016**, *15*, 13–26.
- [2] a) M. W. Tibbit, K. S. Anseth, *Biotech. Bioeng.*, **2009**, *103*, 655–663; b) D. Jhala, R. Vasita, *Polym. Rev.*, **2015**, *55*, 561–595; c) D. Barros, J. F. Amaral, A. P. Pego, *Curr. Top. Med. Chem.*, **2015**, *15*, 1209–1226.
- [3] a) N. A. Peppas, J. Z. Hill, A. Khademhosseini, R. Langer, *Adv. Mater.*, **2006**, *18*, 1345–1360; b) B. V. Slaughter, S. S. Khurshid, O. Z. Fisher, A. Khademhosseini, N. A. Peppas, *Adv. Mater.*, **2009**, *21*, 3307–3329.
- [4] a) A. R. Hirst, B. Escuder, J. F. Miravet, D. K. Smith, *Angew. Chem. Int. Ed.*, **2008**, *47*, 8002–8018; b) R. G. Weiss, *J. Am. Chem. Soc.*, **2014**, *136*, 7519–7530; c) X. Du, J. Zhou, J. Shi, B. Xu, *Chem. Rev.*, **2015**, *115*, 13165–13307; d) E. R. Draper, D. J. Adams, *Chem*, **2017**, *3*, 390–410.
- [5] a) K. J. Skilling, F. Citossi, T. D. Bradshaw, M. Ashford, B. Kellam, M. Marlow, *Soft Matter*, **2014**, *10*, 237–256; b) X. Du, J. Zhou, J. Shi, B. Xu, *Chem. Rev.*, **2015**, *115*, 13165–13307; c) X.-Q. Dou, C.-L. Feng, *Adv. Mater.*, **2017**, *29*, 1604062; d) A. Vashist, A. Kaushik, K. Alexis, R. D. Jayant, V. Sagar, A. Vashist, M. Nair, *Curr. Pharm. Des.*, **2017**, *23*, 3595–3602; e) B. O. Okesola, A. Mata, *Chem. Soc. Rev.*, **2018**, *47*, 3721–3736.
- [6] a) G. A. Silva, C. Czeisler, K. L. Niece, E. Beniash, D. A. Harrington, J. A. Kessler, S. I. Stupp, *Science*, **2004**, *303*, 1352–1355; b) R. G. Ellis-Behnke, Y.-X. Liang, S.-W. You, D. K. C. Tay, S. Zhang, K.-F. So, G. E. Schneider, *Proc. Natl. Acad. Sci. USA*, **2006**, *103*, 5054–5059; c) H. Storrie, M. O. Guler, S. N. Abu-Amara, T. Volberg, M. Rao, B. Geiger, S. I. Stupp, *Biomaterials*, **2007**, *28*, 4608–4618; d) V. M. Tysseling-Mattiace, V. Sahni, K. L. Niece, D. Birch, C. Czeisler, M. G. Fehlings, S. I. Stupp, J. A. Kessler, *J. Neurosci.*, **2008**, *28*, 3814–3823; e) J. P. Jung, A. K. Nagaraj, E. K. Fox, J. S. Rudra, J. M. Devgun, J. H. Collier, *Biomaterials*, **2009**, *30*, 2400–2410; f) S. Kyle, S. H. Felton, M. J. McPherson, A. Aggeli, E. Ingham, *Adv. Healthcare Mater.*, **2012**, *1*, 640–645; g) V. A. Kumar, N. L. Taylor, S. Shi, B. K. Wang, A. A. Jalan, M. K. Kang, N. C. Wickremasinghe, J. D. Hartgerink, *ACS Nano*, **2015**, *9*, 860–868; h) V. A. Kumar, Q. Liu, N. C. Wickremasinghe, S. Shi, T. T. Cornwright, Y. Deng, A. Azares, A. N. Moore, A. M. Acevedo-Jake, N. R. Agudo, S. Pan, D. G. Woodside, P. Vanderslice, J. T. Willerson, R. A. Dixon, J. D. Hartgerink, *Biomaterials*, **2016**, *98*, 113–119.
- [7] a) V. Jayawarna, M. Ali, T. A. Jowitt, A. F. Miller, A. Saiani, J. E. Gough, R. V. Ulijn, *Adv. Mater.*, **2006**, *18*, 611–614; b) T. Liebmans, S. Rydholm, V. Akpe, H. Brismar, *BMC Biotechnol.*, **2007**, *7*, 88.
- [8] a) M. Zhou, A. M. Smith, A. K. Das, N. W. Hodson, R. F. Collins, R. V. Ulijn, J. E. Gough, *Biomaterials*, **2009**, *30*, 2523–2530; b) T. Das, M. Haring, D. Haldar, D. Diaz Diaz, *Biomaterials Sci.*, **2017**, *6*, 38–59.
- [9] a) C. Cheng, M.-C. Tang, C.-S. Wu, T. Simon and F.-H. Ko, *ACS Appl. Mater. Interfaces*, **2015**, *7*, 19306–19315; b) T. Suga, S. Osada, T. Narita, Y. Oishi, H. Kodama, *Mater. Sci. Eng. C: Mater. Biol. Appl.*, **2015**, *47*, 345–350; c) Y. Hu, W. Gao, F. Wu, H. Wu, B. He, J. He, *J. Mater. Chem. B*, **2016**, *4*, 3504–3508; d) E. V. Alakpa, V. Jayawarna, A. Lampel, K. V. Burgess, C. C. West, S. C. J. Bakker, S. Roy, N. Javid, S. Fleming, D. A. Lamprou, J. Yang, A. Miller, A. J. Urquhart, P. W. J. M. Frederix, N. T. Hunt, B. Péault, R. V. Ulijn, M. J. Dalby, *Chem*, **2016**, *1*, 298–319; e) W. Sun, B. Xue, Y. Li, M. Qin, J. Wu, K. Lu, J. Wu, Y. Cao, Q. Jiang, W. Wang, *Adv. Funct. Mater.*, **2016**, *26*, 9044–9052. f) B. Cheng, Y. Yan, J. Qi, L. Deng, Z.-W. Shao, K.-Q. Zhang, B. Lin, Z. Sun, X. Li, *ACS Appl. Mater. Interfaces*, **2018**, *10*, 12474–12484.
- [10] H. Komatsu, S. Tsukiji, M. Ikeda, I. Hamachi, *Chem. Asian J.*, **2011**, *6*, 2368–2375.
- [11] a) G. F. Liu, D. Zhang, C. L. Feng, *Angew. Chem. Int. Ed.*, **2014**, *53*, 7789–7793; b) G. F. Liu, W. Ji, W. L. Wang, C. L. Feng, *ACS Appl. Mater. Interfaces*, **2015**, *7*, 301–307.
- [12] a) S. Ziane, S. Schlaubitz, S. Miraux, A. Patwa, C. Lalande, I. Bilem, S. Lepreux, B. Rousseau, J.-F. Le Meins, L. Latxague, P. Barthélémy, O. Chassande, *Eur. Cells Mater.*, **2012**, *23*, 147–160. b) L. Latxague, M. A. Ramin, A. Appavoo, P. Berto, M. Maisani, C. Ehret, O. Chassande, P. Barthélémy, *Angew. Chem. Int. Ed.*, **2015**, *54*, 4517–4521.
- [13] M. Maisani, S. Ziane, C. Ehret, L. Levesque, R. Siadous, J.-F. Le Meins, P. Chevallier, P. Barthélémy, H. De Oliveira, J. Amédée, D. Mantovani, O. Chassande, *J. Tissue Eng. Regen. Med.*, **2018**, *12*, e1489–e1500.
- [14] a) L. E. Buerkle, H. A. von Recum and S. J. Rowan, *Chem. Sci.*, **2012**, *3*, 564–572; b) A. Rotaru, G. Pricope, T. N. Plank, L. Clima, E. L. Ursu, M. Pinteala, J. T. Davis, M. Barboiu, *Chem. Commun.*, **2017**, *53*, 12668–12671.
- [15] a) J. Liu, Z. Sun, Y. Yuan, X. Tian, X. Liu, G. Duan, Y. Yang, L. Yuan, H.-C. Lin, X. Li, *ACS Appl. Mater. Interfaces*, **2016**, *8*, 6917–6924; b) J. Qi, Y. Yan, B. Cheng, L. Deng, Z. Shao, Z. Sun, X. Li, *ACS Appl. Mater. Interfaces*, **2018**, *10*, 6180–6189.
- [16] a) Y. Ogawa, C. Yoshiyama, T. Kitoaka, *Langmuir*, **2012**, *28*, 4404–4412; b) J. Fitremann, B. Lonetti, E. Fratini, I. Fabing, B. Payre, C. Boule, I. Loubinoux, L. Vaysse, L. Oriol, *J. Coll. Interface Sci.*, **2017**, *504*, 721–730.
- [17] B. O. Okesola, V. M. P. Vieira, D. J. Cornwell, N. K. Whitelaw, D. K. Smith, *Soft Matter*, **2015**, *11*, 4768–4787.
- [18] a) D. J. Cornwell, B. O. Okesola, D. K. Smith, D. K. Smith, *Soft Matter*, **2013**, *9*, 8730–8736; b) B. O. Okesola, D. K. Smith, *Chem. Commun.*, **2013**, *49*, 11164–11166; c) D. J. Cornwell, O. J. Daubney, D. K. Smith, *J. Am. Chem. Soc.*, **2015**, *137*, 15486–15492.
- [19] a) A. Heeres, C. van der Pol, M. C. A. Stuart, A. Friggeri, B. L. Feringa, J. van Esch, *J. Am. Chem. Soc.*, **2003**, *125*, 14252–14253; b) A. Brizard, M. Stuart, K. van Bommel, A. Friggeri, M. de Jong, J. van Esch, *Angew. Chem. Int. Ed.*, **2008**, *47*, 2063–2066; c) S. Fleming, S. Debnath, P. W. J. M. Frederix, N. T. Hunt, R. V. Ulijn, *Biomacromolecules*, **2014**, *15*, 1171–1184; d) S. Himmelein, V. Lewe, M. C. A. Stuart, B. J. Ravoo, *Chem. Sci.*, **2014**, *5*, 1054–1058; e) J. Boekhoven, A. M. Brizard, M. C. A. Stuart, L. Florusse, G. Raffy, A. Del Guerzo, J. H. van Esch, *Chem. Sci.*, **2016**, *7*, 1234–1244.

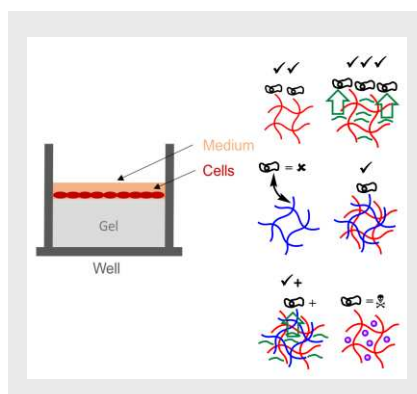
- 7, 6021-6031; f) C. Stubenrauch, F. Giesselmann, *Angew. Chem. Int. Ed.*, **2016**, *55*, 3268-3275.
- [20] V. M. P. Vieira, L. L. Hay, D. K. Smith, *Chem. Sci.*, **2017**, *8*, 6981-6990.
- [21] a) S. E. Sakiyama-Elbert, J. A. Hubbell, *J. Controlled Rel.*, **2000**, *69*, 149-158; b) J. A. Beamish, L. C. Geyer, N. A. Haq-Siddiqi, K. Kottke-Marchant, R. E. Marchant, *Biomaterials*, **2009**, *30*, 6286-6294; c) C. McGann, K. Kiick, K. Heparin-Functionalized Materials in Tissue Engineering Applications. In: *Engineering Biomaterials for Regenerative Medicine*. Ed. S. Bhatia, Springer, New York, pp 225-250, **2012**; d) J. You, D.-S. Shin, D. Patel, Y. Gao, A. Revzin, *Adv. Healthcare Mater.*, **2014**, *3*, 126-132.
- [22] a) L. E. Fechner, B. Albanyan, V. M. P. Vieira, E. Laurini, P. Posocco, S. Pricl, D. K. Smith, *Chem. Sci.*, **2016**, *7*, 4653-4659; b) V. M. P. Vieira, V. Liljeström, P. Posocco, E. Laurini, S. Pricl, M. A. Kostianen, D. K. Smith, *J. Mater. Chem. B*, **2017**, *5*, 341-347.
- [23] a) S. M. Bromfield, A. Barnard, P. Posocco, M. Fermeglia, S. Pricl, D. K. Smith, *J. Am. Chem. Soc.*, **2013**, *135*, 2911-2914; b) S. M. Bromfield, P. Posocco, M. Fermeglia, S. Pricl, J. Rodríguez-López, D. K. Smith, *Chem. Commun.*, **2013**, *49*, 4830-4832.
- [24] D. J. Cornwell, D. K. Smith, *Mater. Horiz.*, **2015**, *2*, 279-293.
- [25] B. O. Okesola, S. K. Suravaram, A. Parkin, D. K. Smith, *Angew. Chem. Int. Ed.*, **2016**, *55*, 183-187.
- [26] a) R. Tiozzo, D. Reggiani, M. R. Cingi, P. Bianchini, B. Osima, S. Calandra, *Thromb. Res.*, **1991**, *62*, 177-188; b) H. Hemeda, J. Kalz, G. Walenda, M. Lohmann, W. Wagner, *Cytotherapy*, **2013**, *15*, 1174-1181.
- [27] a) S. Sakai, I. Hashimoto, K. Kawakami, *J. Biosci. Bioeng.*, **2007**, *103*, 22-26; b) R. Imani, S. H. Emami, P. R. Moshtagh, N. Baheiraei, A. M. Sharifi, *J. Macromol. Sci. B*, **2012**, *51*, 1606-1616.
- [28] a) H. Lv, S. Zhang, B. Wang, S. Cui, J. Yan, *J. Controlled Rel.*, **2006**, *114*, 100-109; b) S. J. Soenen, A. R. Brisson, M. de Cuyper, *Biomaterials*, **2009**, *30*, 3691-3701.

Entry for the Table of Contents (Please choose one layout)

Layout 1:

FULL PAPER

Chemistry Directs Biology – The orthogonal components used in a commercially-relevant self-assembled gel program the biological outcomes.



Vânia M. P. Vieira,^[a] Ana C. Lima,^[b]
Menno de Jong,^[b] David K. Smith^{*[a]}

Page No. – Page No.

**Commercially-Relevant Orthogonal
Multi-Component Supramolecular
Hydrogels for Programmed Cell
Growth**